Compositional Profile of Graded VCSEL DBRs

Fernando Rinaldi and Dietmar Wahl

The compositional profile of graded distributed Bragg reflectors (DBRs) in vertical-cavity surface-emitting lasers (VCSELs) is investigated. Molecular flux measurements allow to determine small differences between the nominal profile and the epitaxially grown structures. These small differences explain completely the suppression of the higher-order satellites in the HRXRD (high-resolution x-ray diffraction) spectra.

1. Introduction

One of the key components of a VCSEL are the DBRs. The simplest Bragg reflector consists of alternating layers of two semiconductors with different refractive indices. It is known that the electrical resistance is drastically reduced by introducing graded composition layers instead of abrupt interfaces in order to avoid band discontinuities [1]. Although this is necessary for electrically pumped devices, such a layer design considerably increases the complexity of the grown structures. It is in the nature of epitaxial growth processes that small deviations between the nominal and the actually grown structures are present. In case of MBE (molecular beam epitaxy), this is mainly caused by the dynamics of the effusion cells. The aim of this work is the detailed measurement of those deviations and their influences on the HRXRD spectra.

2. Actual Compositional Profile

A detailed plot of the nominal composition profile of a DBR period is given in Fig. 1 for the n-doped side. Starting from the first silicon δ-doping sheet (marked with an arrow), one gallium and two aluminum cells are opened together in order to grow $Al_{0.27}Ga_{0.73}As$. Then the composition is ramped linearly with the thickness until $Al_{0.47}Ga_{0.53}As$ is reached. This is done by increasing the aluminum and decreasing the gallium cell temperatures linearly with time. By shutting all the cells, except the one for silicon, a second δ-doping sheet is obtained. In the same way, a ramp from $Al_{0.47}Ga_{0.53}As$ to $Al_{0.90}Ga_{0.10}As$ is followed by the third δ-doping. When the cells are opened again, their temperature is kept constant and an $Al_{0.90}Ga_{0.10}As$ layer of constant composition is grown. After that, the AlAs/AlGaAs fraction is symmetrically ramped down, but without introducing δ-doping, until an aluminum fraction of 20 percent is reached and kept constant for 37 nm. The cells are then shut for δ-doping and the cycle starts again.

As will be shown in detail in the following, the HRXRD spectra of grown VCSELs show evidence that the compositional profile of the DBRs differs from the nominal one. There

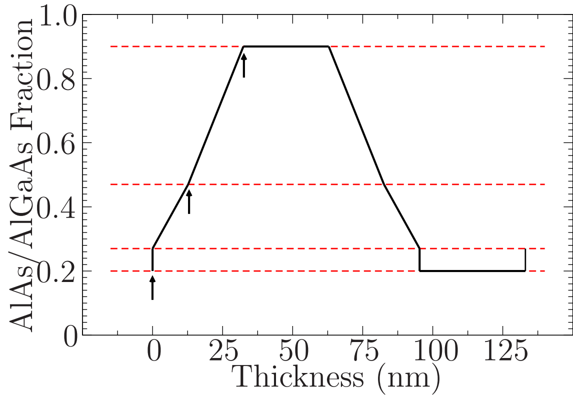

Fig. 1: Nominal compositional profile of a n-doped DBR period in a 850 nm VCSEL. The arrows represent δ-doping. Four linearly graded layers per period are present.

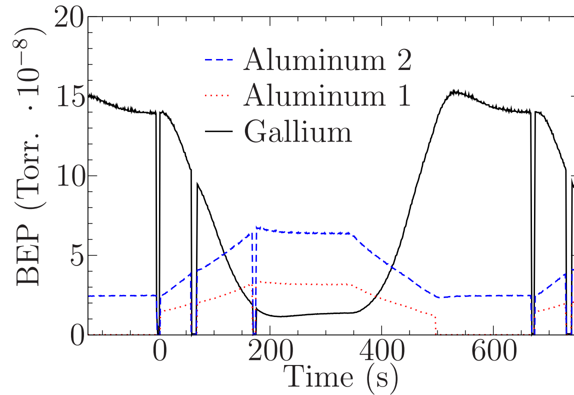

Fig. 2: Measured fluxes from the three effusion cells used to grow the nominal structure shown in Fig 1. One DBR period is grown in approximately 670 s.

are several causes for this behavior, considering that during the ramps, the cells are programmed to change their temperature linearly with time. In fact, the fluxes are not linear functions of the temperature, and the effusion cells have a certain response time and a specific dynamic behavior.

One has to mention that in the VCSEL design, there is no particular reason to choose linearly graded profiles, and so there is also no reason to try to correct the real compositional profile in order to better match the one shown in Fig. 1. In fact, the specific profile influences the maximum reflectivity and the width of the stop-band, which is always present as long as the periodicity of the structure is maintained. Small deviations of the profile do not affect the optical reflectivity spectrum significantly. It follows that one can accidentally grow graded DBRs with high reflectivity at the design wavelength using wrong growth rates for the different cells. But this can cause unintentional detuning of the laser cavity or affect other features of the structure.

Precise data of the profile can be obtained by measuring the fluxes of each effusion cell involved in the growth process when these are driven in the same way as during growth. For these measurements, a Bayard–Alpert ionization gauge [2] was located at the substrate position. The growth rate, that is proportional to the measured beam equivalent pressure (BEP), can be acquired as a function of time for each cell separately. The resulting fluxes from the gallium and the two aluminum cells were successively measured. The data, expressed in BEP, are plotted in Fig. 2, where one can recognize the occurrence of the three δ-doping sheets, when all the cells are shut and the BEPs drop to zero. Those flux drops can be used to synchronize the three data sets and display them in the diagram according to the growth recipe. To achieve the desired grading of the aluminum concentration, the gallium flux increases while the aluminum fluxes decrease and vice versa. Unlike the aluminum cells, the gallium cell shows a big flux overshoot approximately 530 s after the period has started. This proves that relevant effects are arising from the response of the cells to the transients. Using the calibration table, it is possible to convert the fluxes into

growth rates. The AlAs/AlGaAs fraction c as a function of time is given by

$$c(t) = \frac{G_{\mathrm{Al1}}(t) + G_{\mathrm{Al2}}(t)}{G_{\mathrm{Al1}}(t) + G_{\mathrm{Al2}}(t) + G_{\mathrm{Ga}}(t)}\,, \tag{1}$$

where $G(t)$ represent the growth rates of AlAs or GaAs as a function of time for a specific cell. Integrating the total growth rate over time, one gets the grown thickness d at a specific time t as

$$d(t) = \int_0^t (G_{\mathrm{Al1}}(t') + G_{\mathrm{Al2}}(t') + G_{\mathrm{Ga}}(t'))\,\mathrm{d}t'\ . \tag{2}$$

Eliminating t from (1) and (2), one gets the compositional profile $c(d)$, which is shown in Fig. 3 in comparison with the nominal one. The $c(d)$ measured for four periods are shown in Fig. 4, where the layer reproducibility and so the periodicity of the DBR are strictly confirmed. A simplified sample made of 34 n-doped periods was grown to analyze the periodic structure in detail. The HRXRD spectra are shown in Fig. 6. One can see that the simulation based on the linearly graded compositional profile shows high-order satellite peaks that are not present in the measurements. From the kinematical theory of scattering, the satellite peaks are related to the Fourier components of the electron density of the periodic superlattice; they represent its structure factor. The suppression of the satellites is caused by the smoother profile. Despite almost all VCSELs have graded composition profiles to reduce the electrical resistance, the HRXRD spectra of the DBRs are seldom analyzed in literature. The problem is marginally treated in [3] and in more detail in [4], where the idea to mimic smooth profiles by a biparabolic function is introduced.

The biparabolic profile is defined as

$$c(x) = c_1 + \frac{(c_2 - c_1)(x - d_1)^2}{(d_2 - d_1)^2} \qquad \text{for} \qquad d_1 \le x \le d_2 \tag{3}$$

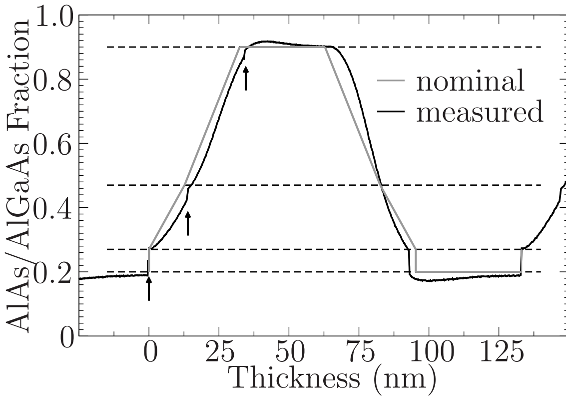

Fig. 3: Comparison between the nominal and measured compositional profiles in a 850 nm VCSEL DBR period. The arrows represent δ-doping. The experimental profile is obtained by flux measurements.

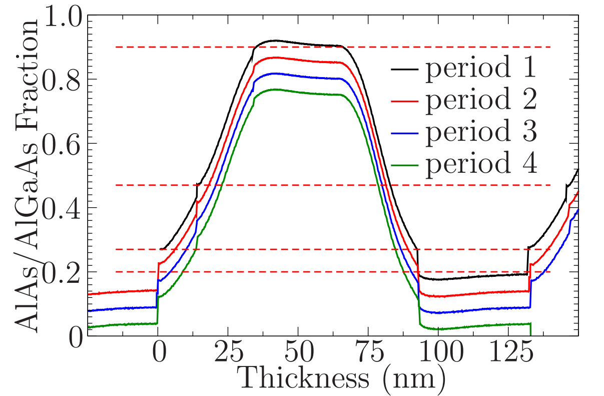

Fig. 4: Comparison between the profiles of four adjacent DBR periods obtained from flux measurements. For clarity, the profiles are shifted by 5 % each.

and

$$c(x) = c_3 + \frac{(c_2 - c_3)(x - d_3)^2}{(d_3 - d_2)^2} \qquad \text{for} \qquad d_2 \le x \le d_3 \ , \tag{4}$$

where the indices 1 and 3 refer to the starting and final points, respectively, and the index 2 refers to the junction point of the two parabolas, as can be seen in Fig. 5. The continuity of the profile is directly given by (3) and (4), and six parameters are necessary to define the curve. The continuity of the first derivative reduces the free parameters to five and requires

$$\frac{c_3 - c_2}{d_3 - d_2} = \frac{c_2 - c_1}{d_2 - d_1} \ . \tag{5}$$

In Figs. 6, 7, and 8, the measured and simulated HRXRD spectra for the test sample and for a complete VCSEL structure are plotted. In both cases one can see that the linearly graded nominal profile is not adequate to fit the spectra. From Fig. 1, it is inferred that, because of its symmetry, 8 parameters are needed to fit the nominal profile. Using a biparabolic profile, like in Fig. 5, also 8 parameters are needed to fit the complete profile, which is also considered symmetric. In fact, condition (5) was not used here. The comparisons in Figs. 7 and 8 indicate that at least 15 lamellae are needed for a satisfactory fit. As seen in Fig. 5, a good approximation of the measured profile is then obtained.

It is important to point out that it is impractical to obtain the compositional profile by flux measurements before the growth of each sample. As shown, this can be extracted by HRXRD, giving precise information that can be used for the next growth run.

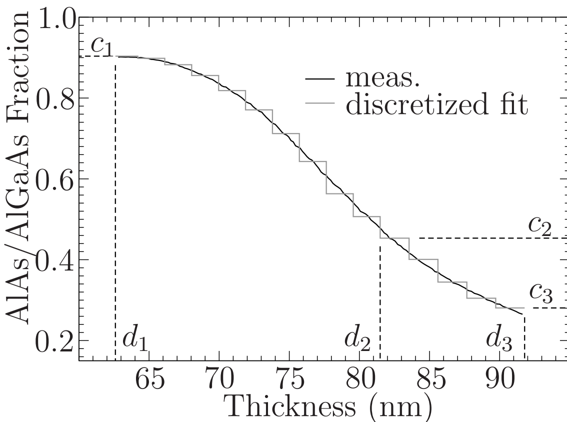

Fig. 5: Discretized biparabolic composition profile used to fit the VCSEL spectra in Figs. 7 and 8, as well as the profile obtained by flux measurements. The number of used lamellae is 15.

3. Acknowledgement

We thank Shunyi Li for his help with the HRXRD measurements and the spectra fits using a commercial x-ray diffraction dynamic theory simulation tool.

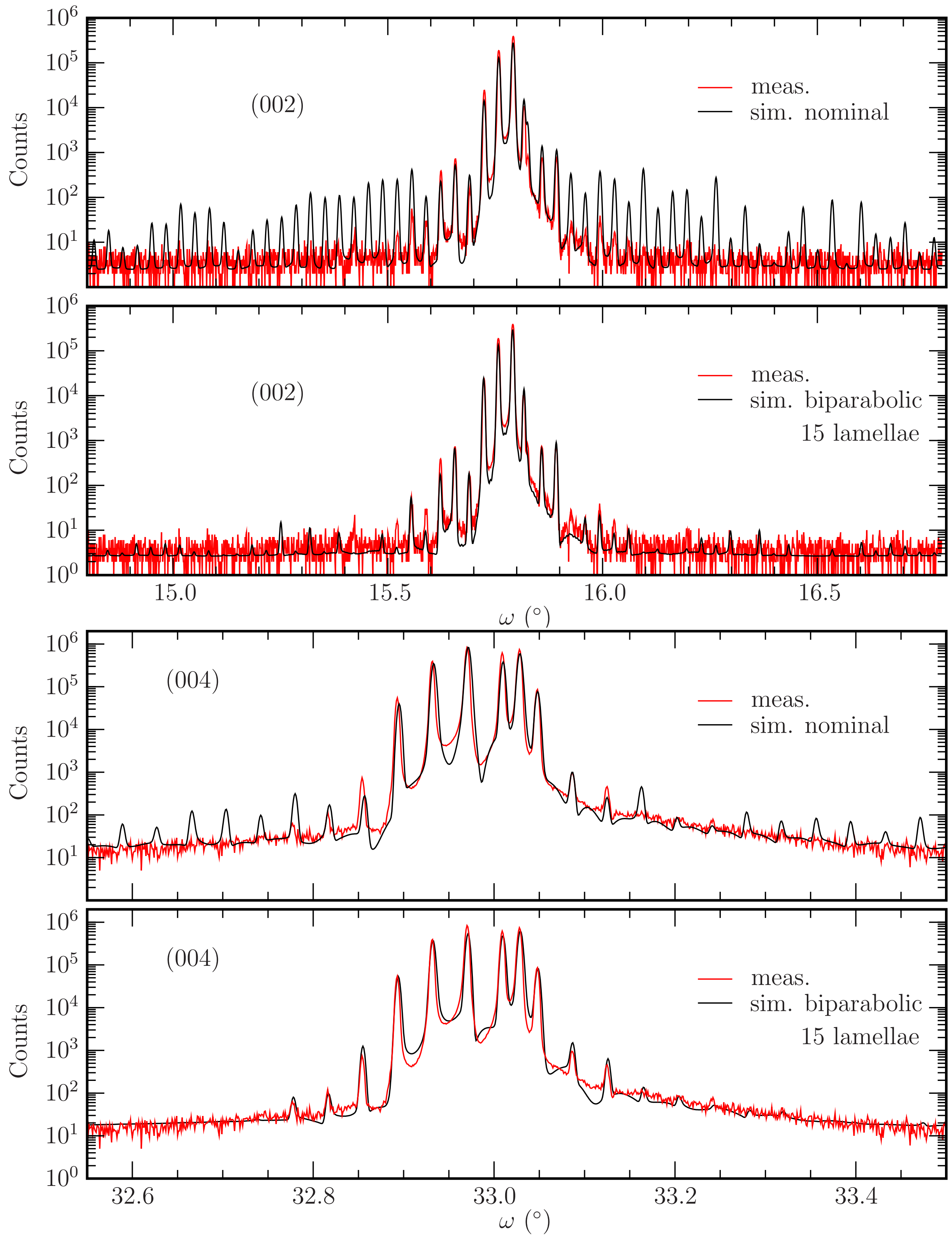

Fig. 6: HRXRD (002) and (004) spectra of the 34 periods n-doped DBR. The corresponding simulations are made both with nominal (linearly graded) and discretized biparabolic profiles.

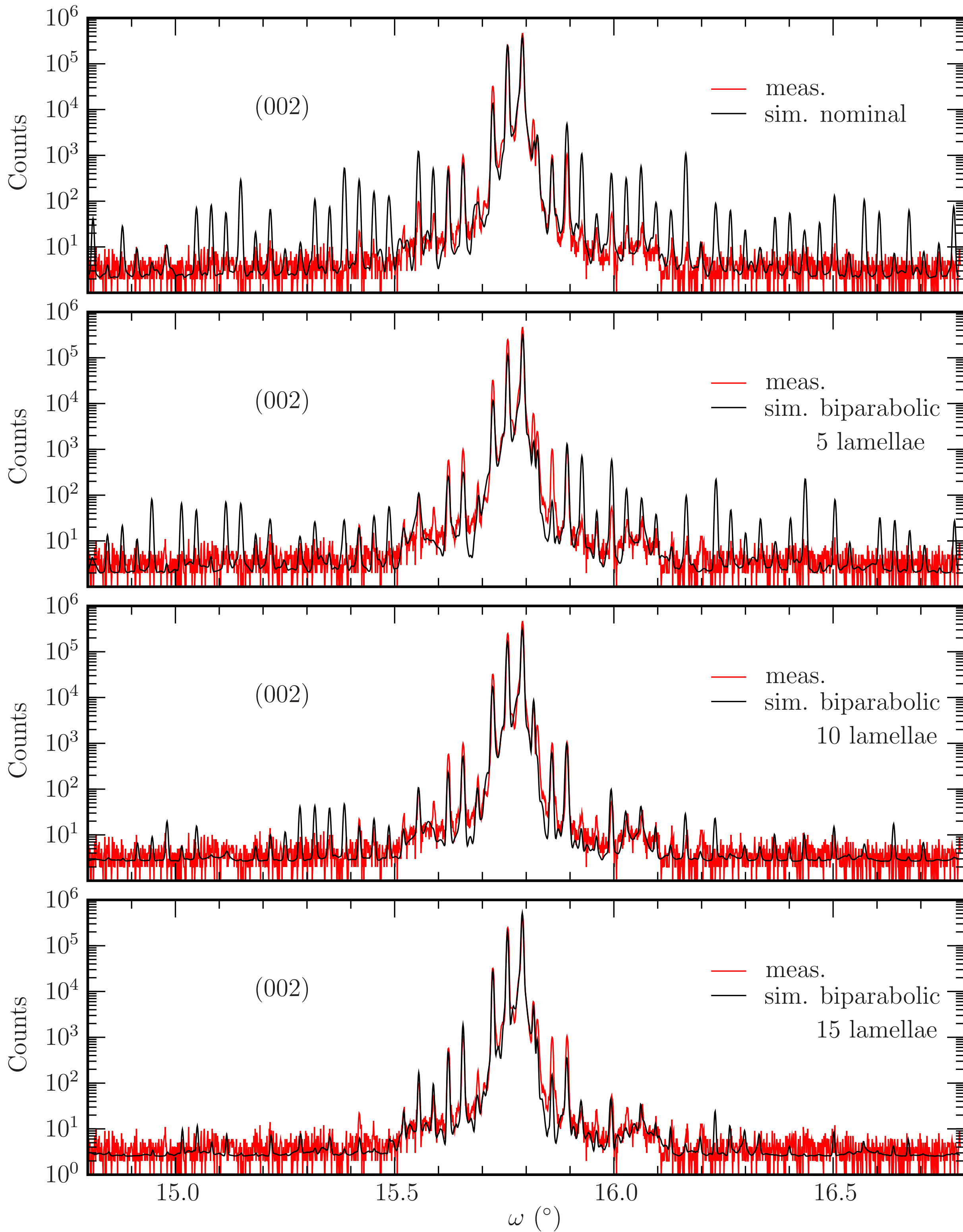

Fig. 7: HRXRD (002) spectra of a complete 850 nm VCSEL structure. The corresponding simulations use nominal (linearly graded) and biparabolic profiles with 5, 10, and 15 lamellae.

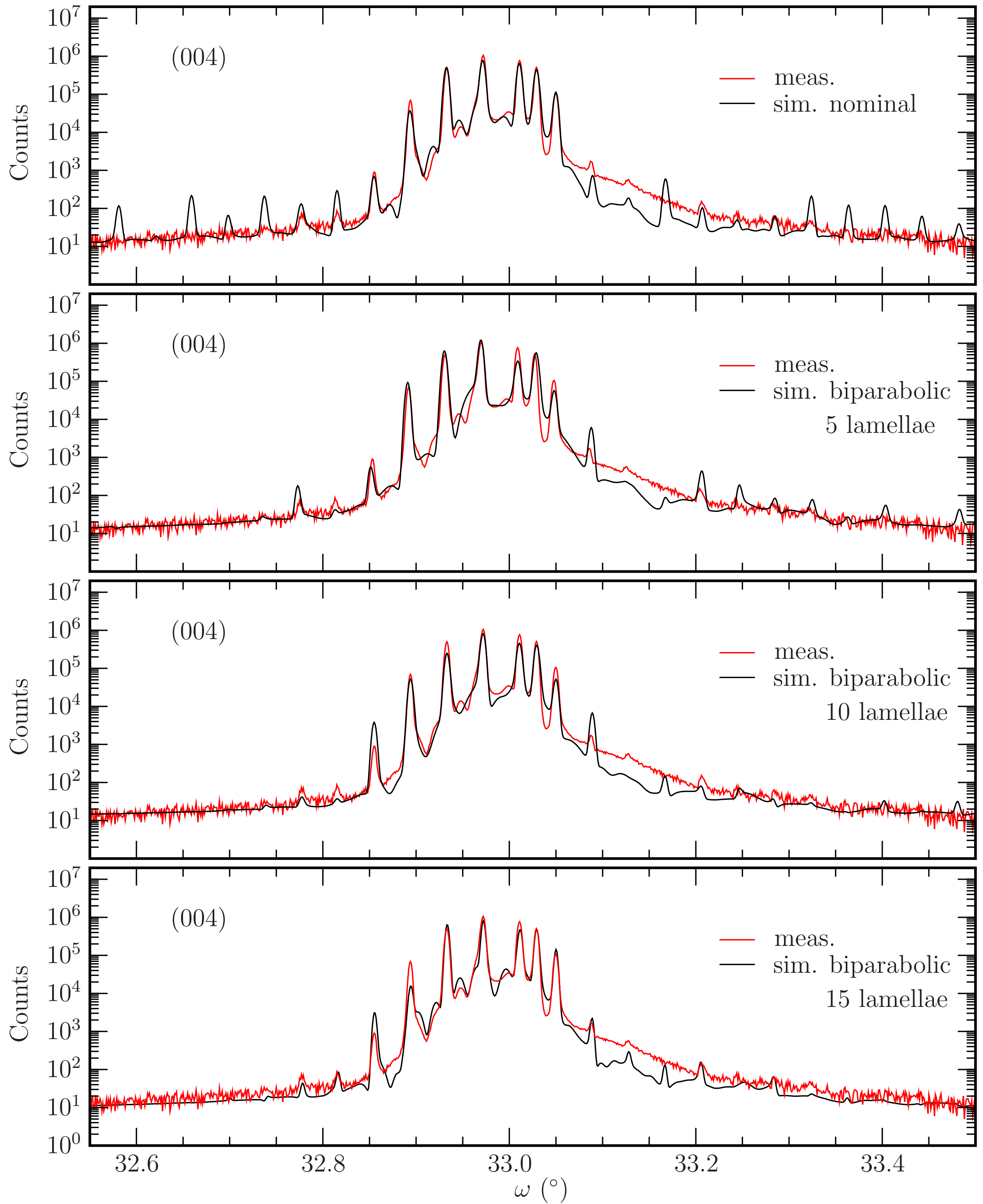

Fig. 8: Same as Fig. 7, here referring to the HRXRD (004) reflection.

References

[1] K. Tai, L. Yang, Y.H. Wang, J.D. Wynn, and A.Y. Cho, "Drastic reduction of series resistance in doped semiconductor distributed Bragg reflectors for surface-emitting lasers", *Appl. Phys. Lett.*, vol. 56, pp. 2496–2498, 1990.

[2] R.K. Fitch, "Total pressure gauges", *Vacuum*, vol. 37, pp. 637–641, 1987.

[3] P. Kidd, "Investigation of the precision in x-ray diffraction analysis of VCSEL structures", *J. Mat. Sci.: Mat. Electron.*, vol. 14, pp. 541–550, 2003.

[4] S.G. Patterson, G.S. Petrich, R.J. Ram, and L.A. Kolodziejski, "X-ray diffraction analysis of bandgap-engineered distributed Bragg reflectors", *J. Electron. Mat.*, vol. 28, pp. 1081–1083, 1999.